*Bioscience Reports* (2018) **38** BSR20180536
https://doi.org/10.1042/BSR20180536

PORTLAND PRESS

Research Article

# Differential expression of NPM, GSTA3, and GNMT in mouse liver following long-term *in vivo* irradiation by means of uranium tailings

**Lan Yi[1,2,*], Hongxiang Mu[2,*], Nan Hu[1,*], Jing Sun[2], Jie Yin[1,2], Keren Dai[2], Dingxin Long[1] and Dexin Ding[1]**

[1]Key Discipline Laboratory for National Defense for Biotechnology in Uranium Mining and Hydrometallurgy, University of South China, Hengyang 421001, Hunan Province, P.R. China; [2]Institute of Cytology and Genetics, College of Pharmaceutical and Biological Science, University of South China, Hengyang 421001, Hunan Province, P.R. China

**Correspondence:** Dexin Ding (dingdxzzz@163.com)



Uranium tailings (UT) are formed as a byproduct of uranium mining and are of potential risk to living organisms. In the present study, we sought to identify potential biomarkers associated with chronic exposure to low dose rate γ radiation originating from UT. We exposed C57BL/6J mice to 30, 100, or 250 μGy/h of gamma radiation originating from UT samples. Nine animals were included in each treatment group. We observed that the liver central vein was significantly enlarged in mice exposed to dose rates of 100 and 250 μGy/h, when compared with nonirradiated controls. Using proteomic techniques, we identified 18 proteins that were differentially expressed (by a factor of at least 2.5-fold) in exposed animals, when compared with controls. We chose glycine N-methyltransferase (GNMT), glutathione S-transferase A3 (GSTA3), and nucleophosmin (NPM) for further investigations. Our data showed that GNMT (at 100 and 250 μGy/h) and NPM (at 250 μGy/h) were up-regulated, and GSTA3 was down-regulated in all of the irradiated groups, indicating that their expression is modulated by chronic gamma radiation exposure. GNMT, GSTA3, and NPM may therefore prove useful as biomarkers of gamma radiation exposure associated with UT. The mechanisms underlying those changes need to be further studied.

## Introduction

The biological effects of chronic low dose rate on normal tissues have attracted much attention in recent years [1]. Many studies have shown that sustained low dose radiation (LDR) can cause harm to organisms, such as chromosome aberrations [2], genomic instability [3], cell inactivation [4], and tumorigenicity [5]. Persistent detrimental effects for the cardiovascular system have also been reported [6]. There is also evidence to suggest that ionizing radiation, in addition to other factors, may have an impact on the pathology of neurodegenerative diseases such as Alzheimer's [7]. However, there is also a large body of literature describing the beneficial effects of LDR exposure, such as the prevention of doxorubicin-induced cardiotoxicity by suppressing mitochondrial-dependent oxidative stress and apoptosis signaling [8]. Research has shown that LDR can activate the adaptive immune response, promoting immune-dependent tumor inhibition [9].

Recently, there has been a growing interest in environmental and public health impact of uranium tailings (UT), with uranium being shown as the cause of irreversible impacts on the surrounding environment [10]. UT can cause environmental pollution [11,12] and represent a hazard for humans [13,14]. Research has shown that chemicals and radionuclides present in the tailings influence soil properties and microbial diversity [15]. UT can lead to human disease and health complications after occupational or environmental exposure [16]. Thus, it is very important to develop biomarkers that can be used to assess risks associated with UT.

[*] These authors contributed equally to this work.

Received: 07 April 2018
Revised: 21 July 2018
Accepted: 26 July 2018

Accepted Manuscript Online: 30 July 2018
Version of Record published: 17 October 2018

*Bioscience Reports* (2018) **38** BSR20180536
https://doi.org/10.1042/BSR20180536

Proteomics provides information on the structure, expression, and function of proteins. It has been applied in fields such as clinical diagnosis [17-19] and tumor marker discovery [20]. Proteomics can be used to analyze the post-translational modifications of proteins. It is used to identify and quantify the overall protein content of a cell, tissue or an organism, and it is one of the most informative methodologies available for comprehending gene function [21].

Through proteomics analysis, our previous research identified differentially expressed proteins in the liver tissues of mice that had received different doses of Cs-137 radiation for 90 and 180 days [22,23]. It is well known that $\alpha$ and $\gamma$ radiations associated with UT also have the potential to harm workers. In the present study, we used UT as a low dose rate source to irradiate C57BL/6J mice. The purpose of the study was to use quantitative proteomics to identify liver biomarkers of radiation exposure for the early detection of UT-associated health effects. At first, we used quantitative proteomics to identify those proteins in mouse liver tissue that are differentially expressed. Then, we further analyzed selected proteins to evaluate if they could potentially be used as biomarkers of radiation exposure.

# Materials, design, and methods

## Mice and irradiation

We purchased 6-to 7-week-old male C57BL/6J mice from the Hunan Slack King of Laboratory Animal Co., Ltd. (Changsha, China). We bred the mice in the Animal Department of the University of South China. To initiate the study, we used 36 six- to seven-week-old mice that were randomly distributed between the four experimental groups. Three groups were exposed for 500 days to whole-body radiation from UT at dose rates of 30, 100, and 250 μGy/h. The UT dose rate was monitored precisely using a $\gamma$ detector (Shanghai Renri Radiation Protection Equipment Co., Ltd., Shanghai, China). Nonirradiated mice, which were used as controls, were treated the same as the irradiated mice. The exposed mice were placed above the UT for 22 h per day. The remaining 2 h were used for clinical observations of the test animals, room cleaning and bedding replacement, and to provide a fresh supply of food and water. We used a lead brick to shield the nonirradiated mice. The dose rate received by the nonirradiated matched group was less than 0.2 μGy/h. Mice were housed at a temperature of 22–26°C, and humidity of 45–70%. After 500 days, mice were killed by cervical dislocation. The liver tissue was harvested, washed with PBS, and snap-frozen at −80°C for later use. We conducted all experimental procedures in accordance with the guidelines approved by the Institutional Animal Care and Use Committee of the University of South China, Hunan, China.

## Hematoxylin and eosin staining of liver tissues

The liver tissues were fixed in 10% neutral formalin solution, and embedded in paraffin, and then cut into 4-μm-thick sections. The sections transferred onto glass slides. The slides were immersed in $H_2O$ for 30 s and dipped in Mayer's hematoxylin and agitated for 30 s. The slides were rinsed in $H_2O$ for 60 s and then stained with 1% eosin Y solution for 10–30 s with agitation. The sections were dehydrated with 95 and 100% alcohol for 30 s each, and then the alcohol was extracted with xylene. One or two drops of mounting medium was added and covered with a cover slip. All reagents came from Shanghai Biotechnology.

## Protein extraction and quantification

We homogenized whole frozen mouse livers to a powder using a liquid nitrogen-cooled pestle and mortar. The tissue powder was then rehydrated in lysis buffer and subjected to sonication. The resulting lysate was centrifuged at 1200 ***g*** for 20 min at 4°C, the supernatant was then collected and incubated on a shaking table at 4°C for 1 h. We used the Bicinchoninic Acid (BCA) Protein Assay Kit (Beijing ComWin Biotech Co., Ltd., Beijing, China) to quantify the proteins, and the supernatants were stored at −20°C.

## Two-dimensional gel electrophoresis, staining, and image analysis

We extracted the total protein from mouse liver of four groups for two-dimensional gel electrophoresis (2-DE) analysis [24]. After electrophoresis, Coomassie brilliant blue was used to stain gels, and we used PD Quest software (Bio-Rad, CA, U.S.A.) to perform background subtraction, spot detection, spot matching, and quantification. Each spot was analyzed with six gel images: three used the matched group and three used a group with a different dose of irradiation. We used a Powerlook1100, scanner, and UMAX (Taipei, China) to obtain gel images at 300 dots per inch (dpi), and then used GE Healthcare ImageMaster™ 2D Platinum 5.0 software (Stockholm, Sweden) to analyze the gel images. We used the 2D Elite Automatic Spot Detection Program to detect spots to calculate spot volumes with respect to normalization and background values. The percentage volume of gel occupied by each spot was determined by

**Table 1 The primer sequences for GNMT, GSTA3, NPM, and *Actb***

| Gene | Primer sequence | Length |
|---|---|---|
| *Gnmt* | F: 5′AACTGGTTGACGCTGGACAA-3′ | 133 bp |
| | R: 5′TGTTCTTTAGTGCCAGCCGG-3′ | |
| *Gsta3* | F: TCGACGGGATGAAACTGGTG | 128 bp |
| | R: CAGATCCGCCACTCCTTCTG | |
| *Npm1* | F: GAAGTGTGGTTCAGGGCCTG | 122 bp |
| | R: ATCGCTTTCCAGACATGCCT | |
| *Actb* | F: 5' GCCAACCGTGAAAAGATGAC 3' | 541 bp |
| | R: 5' GAGGCATACAGGGACAGCAC 3' | |

comparing spot volume with total gel volume. Student's *t* test was used to determine the differentially expressed protein spots between control and experimental groups, spots with a fold-change of $\geq$2.5 and a *P*-value of $<$0.05 were considered statistically significant.

## *In situ* protein digestion and matrix-assisted laser desorption/ionization time of flight mass spectrometry

Prior to mass spectrometry analysis, protein spots were subjected to enzymatic hydrolysis followed by destaining and drying. Two standards were used to obtain the final peptide mass fingerprinting (PMF) and to calibrate the spectrum. The internal standard was the trypsin self-degradation ion peak and matrix peak. The external standard used was the Peptide Calibration Standard II from Bruker Daltonics, Inc. (Massachusetts, U.S.A.). Peak list generation was conducted using the GPS Explorer Software Version 3.6 (Applied Biosystems, Foster, U.S.A.), and searches against the international protein index (IPI) mouse protein databases were performed using the Mascot database search algorithms (version 2.1, Matrix Science Ltd). The identification of proteins by PMF using Mascot was carried out using parameters similar to those used for the IPI mouse database. We used the IPI mouse protein and Mascot database search engine to determine gene ontology categories, protein functions, and gene names. Proteins with scores $>$55 and located outside of the green shadow were considered to be meaningful 'hits' in the present study.

## Real-time polymerase chain reaction

Real-time PCR was performed to evaluate changes in glycine N-methyltransferase *(Gnmt)*, glutathione S-transferase A3 *(Gsta3)*, and nucleophosmin *(Npm1)* gene expression. *Actb* expression was used as an internal control. All primer sequences were designed using Primer 5.0 software and synthesized by Sangon Biotech (Shanghai, Japan). Primer sequences are shown in Table 1.

Total RNA was extracted from tissue samples using the High Pure RNA Tissue Kit (Omega Company, Norcross, U.S.A.) according to the manufacturer's instructions. A NanoDrop ND-1000 (Omega Company) was used to measure RNA purity and concentration. The Transcriptor First Strand cDNA Synthesis Kit (Roche) was used to generate cDNA according to the manufacturer's instructions. Briefly, total RNA was incubated with 1 μl oligo (dT)18 at 70°C for 3 min and cooled to 37°C for an additional 10 min. Subsequently, 4 μl dNTP mixture, 2 μl 10× RT reaction buffer (DBI Bioscience, Ludwigshafen, Germany), 200 units of Moloney murine leukemia virus reverse transcriptase, and 1 μl of RNase inhibitor were added and first strand cDNA synthesis then performed by incubating the mixture at 37°C for 1 h and then at 95°C for 5 min, followed by cooling on ice. Reverse-transcription and real-time PCR were performed as described previously [22]. Thermocycling parameters involved a 95°C incubation for 5 min and then 40 cycles of a 95°C incubation for 10 s, a 59°C incubation for 15 s and a 72°C incubation for 20 s. The samples were heated from 72–99°C to provide a melt curve analysis.

## Western blotting

The BCA protein quantification assay was used to measure liver total protein from irradiated and nonirradiated mice. Total protein (50 μg) was mixed with loading buffer at a 5:1 ratio. Samples were boiled for 5 min at 100°C to denature proteins, and then resolved by SDS–PAGE using a 10% polyacrylamide gel. Proteins were subsequently transferred onto a PVDF membrane for 2 h at 4°C and then blocked with tris-buffered saline–0.1% Tween 20 (TBST) containing 5% nonfat dry milk for 2 h at room temperature. After blocking, the membrane was incubated with primary antibody for 12 h at 4°C. NPM and GSTA3 antibodies were from Abcam (Cambridge, U.K.). The GNMT antibody was from Santa Cruz Biotechnology (California, U.S.A.). The PVDF membrane was washed five times (10 min each) with TBST

*Bioscience Reports* (2018) **38** BSR20180536
https://doi.org/10.1042/BSR20180536

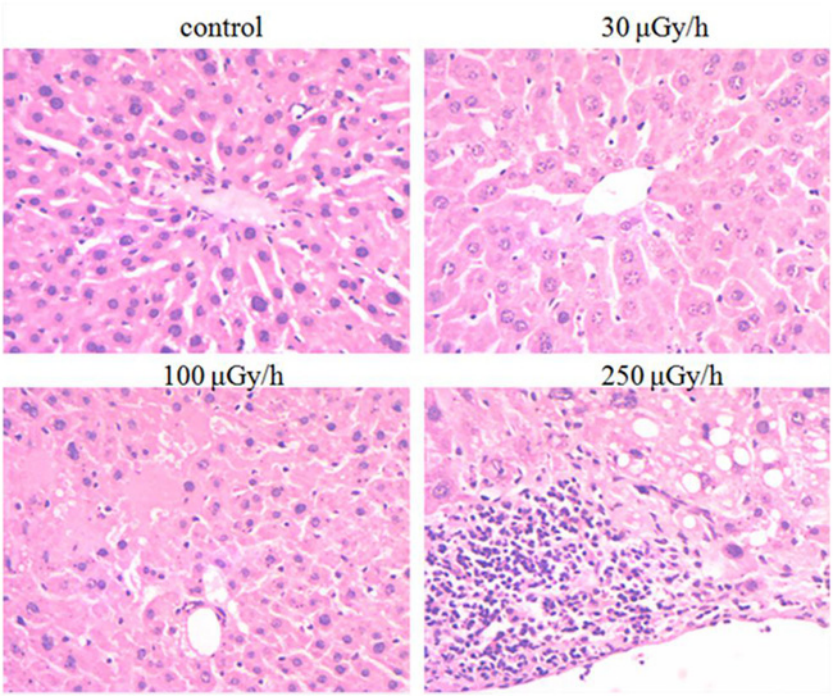


**Figure 1. Morphology of liver tissues obtained from mice that were chronically exposed to 30, 100, and 250 μGy/h**

and then incubated for 1 h with secondary antibody (Beyotime Biotechnology, ShangHai, China). Antibody binding was detected by enhanced chemiluminescence (ComWin Biotech Co., Ltd., Beijing, China). Chemical luminescence reagent was used to detect Western blotting (WB) results.

## Statistics

All statistical analyses were performed with the SPSS statistical software, version 18.0. And the results were presented as S.D. $\pm$ mean. We used $t$-test to test the differences between groups and $P<0.05$ was considered significant.

# Results

## Morphological changes in the liver tissues of mice that were exposed to different radiation dose rates originating from UT

Histological analysis of mouse liver tissue obtained from animals that received different dose rates of UT irradiation over a 500 day period was performed to determine whether any gross change in tissue morphology had occurred. As shown in Figure 1, the central vein was slightly dilated in the 30 μGy/h irradiated group, when compared with the matched control group. We did not observe other pathological changes in the liver tissues. Central vein dilation was obvious in the 100 and 250 μGy/h groups. Necrosis was also prominent in the liver tissues of the 250 μGy/h group, and there was also some interstitial fibrosis and steatosis.

## Comparative proteomics analysis of nonirradiated and irradiated mice by 2-DE

We detected more than 600 protein spots in each gel. There were 10, 11, and 17 spots above the 2.5-fold-change threshold in the 30, 100, and 250 μGy/h experimental groups, respectively, when compared with the matched control group.

## Mass spectrometry and bioinformatics analysis of the differentially expressed protein spots

We used matrix-assisted laser desorption/ionization time of flight mass spectrometry (MALDI-TOF-MS) to analyze the 29 protein spots that satisfied our selection criteria ($\geq$2.5-fold changes in expression with obvious error dots

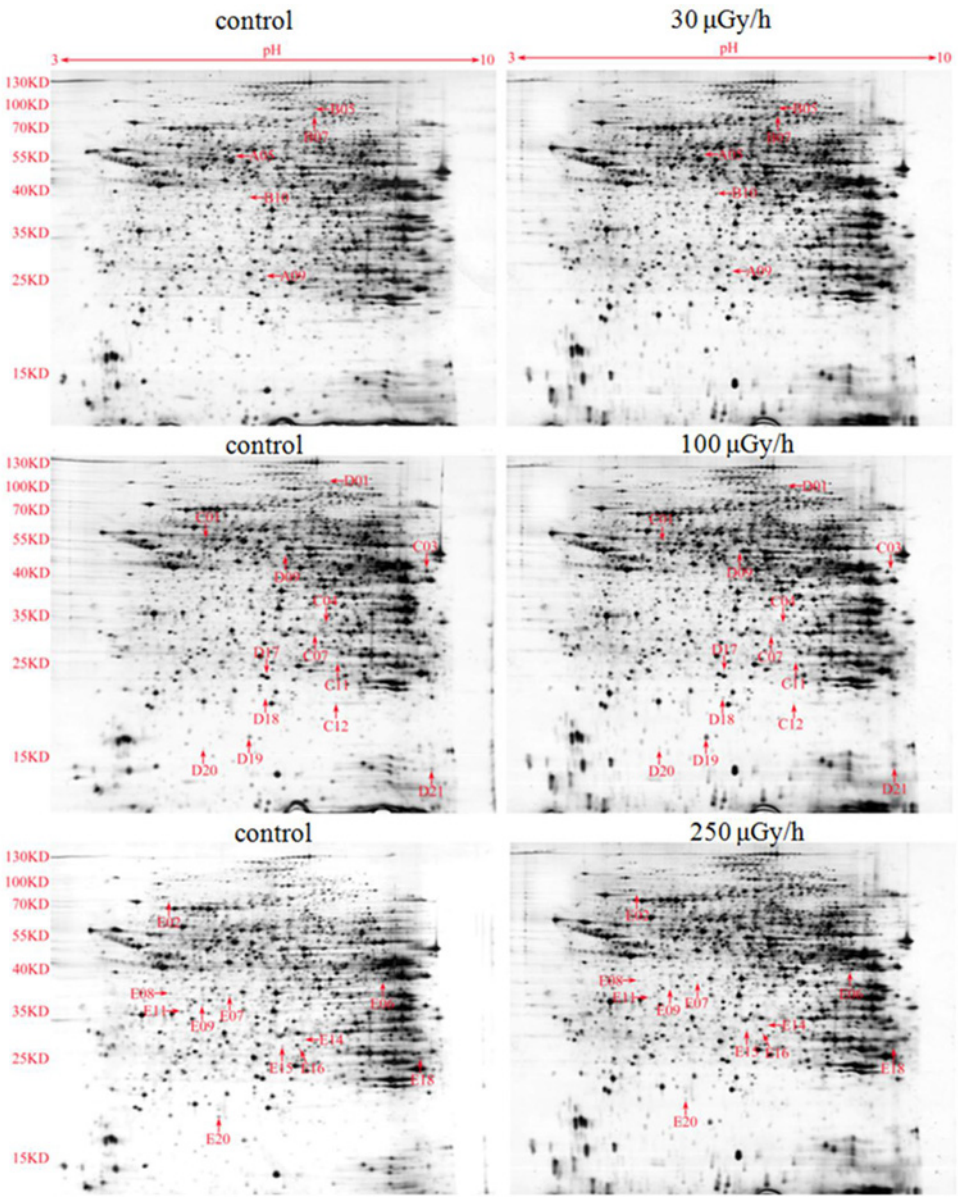


**Figure 2. 2-DE of total liver protein obtained from mice that were chronically exposed to 30, 100, and 250 μGy/h**

removed), and then performed a database search to identify individual proteins. Figure 2 shows 29 spots with accurate spectral information provided by the PD Quest Software. Figure 3 provides the peptide mass finger print of spot number C04 obtained by MALDI-TOF-MS. The SWISS-PROT and NCBI databases were used to analyze 24 spots. Protein spot number C04 was identified as GNMT, with a score of 236 and a sequence coverage of 45%. Eighteen protein spots had a score of more than 55, and their data are summarized in Table 2.

## Real-time polymerase chain reaction verification

We chose GNMT, GSTA3, and NPM for further analysis and performed real-time PCR to verify that changes observed at the protein level were reflected by corresponding changes in gene expression. Proteomics had revealed that GNMT was up-regulated in both the 100 and 250 μGy/h irradiated groups, that GSTA3 was down-regulated in the 100 μGy/h irradiated group, and that NPM was up-regulated in the 250 μGy/h irradiated group.

As shown in Figure 4, GNMT mRNA expression was increased in both the 100 and 250 μGy/h irradiated groups, when compared with controls ($P<0.05$), a finding that was consistent with the proteomics analysis. GSTA3 mRNA

*Bioscience Reports* (2018) **38** BSR20180536
https://doi.org/10.1042/BSR20180536

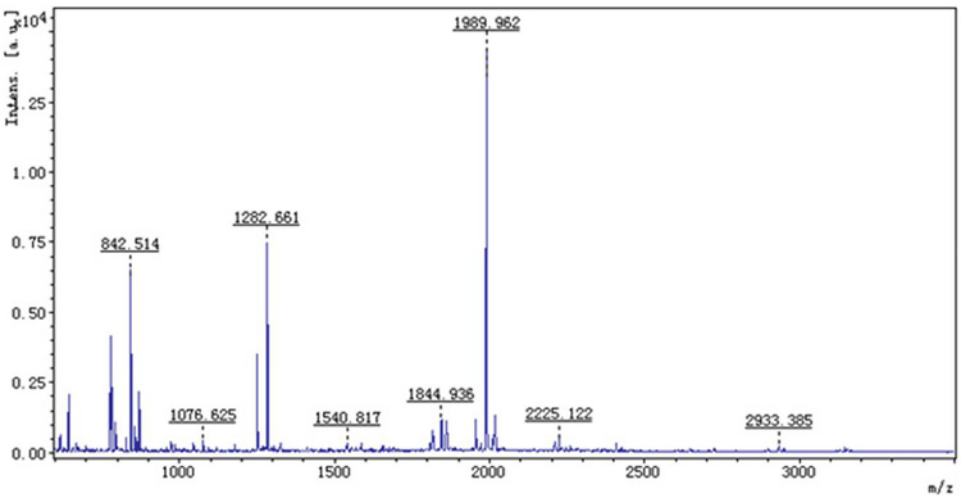


**Figure 3. PMF print of protein spot C04 obtained using MALDI-TOF-MS**

**Table 2 Differentially expressed proteins identified by MALDI-TOF-MS**

| Spot | Entry name | Protein identified | Score | Mr (Da) | IP | Squence coverge | Function |
|---|---|---|---|---|---|---|---|
| 09 | IDI1_MOUSE | Isopentenyl-diphosphate Delta-isomerase 1* | 166 | 26615 | 5.79 | 37% | Catalysis |
| B07 | CPSM_MOUSE | Carbamoyl-phosphate synthase [ammonia], mitochondrial† | 235 | 165711 | 6.48 | 8% | Catalysis |
| C01 | K2C8_MOUSE | Keratin, type II cytoskeletal 8* | 172 | 54531 | 5.7 | 22% | Cytoskeletal protein/protection |
| C04 | GNMT_MOUSE | Glycine N-methyltransferase * | 236 | 33111 | 7.1 | 45% | Metabolic enzyme regulates lipid and glucose homeostasis |
| C07 | D3YU12_MOUSE | NmrA-like family domain-containing protein 1* | 150 | 33232 | 6.32 | 25% | Domain protein |
| C11 | CMBL_MOUSE | Carboxymethylenebutenolidase homolog* | 140 | 28226 | 6.71 | 32% | Hydrolases |
| C12 | QOR_MOUSE | Quinone oxidoreductase* | 177 | 35531 | 8.18 | 18% | Chemical carcinogen metabolizing enzyme |
| D18 | GSTP1_MOUSE | Glutathione S-transferase P 1† | 265 | 23765 | 7.68 | 42% | Liver detoxification |
| D19 | GSTA3_MOUSE | Glutathione S-transferase A3† | 171 | 25401 | 8.76 | 55% | Carcinogenesis |
| D20 | A0A087WQI6_MOUSE | Glutathione S-transferase (Fragment)† | 60 | 15359 | 5.38 | 8% | Liver detoxification |
| D21 | BHMT1_MOUSE | Betaine–homocysteine S-methyltransferase 1† | 172 | 45448 | 8.01 | 20% | Zinc-dependent enzyme/catalysis |
| E08 | NPM_MOUSE | Nucleophosmin* | 72 | 32711 | 4.62 | 23% | Cell growth, proliferation, and apoptosis/carcinogenesis |
| E09 | ALBU_MOUSE | Serum albumin* | 198 | 70700 | 5.75 | 21% | Maintaining the oncotic pressure/free radical scavenging |
| E11 | TBB5_MOUSE | Tubulin β-5 chain* | 136 | 50095 | 4.78 | 14% | Cytoskeletal protein |
| E14 | HUTH_MOUSE | Histidine ammonia-lyase* | 207 | 72897 | 5.94 | 20% | Catalysis |
| E15 | GNMT_MOUSE | Glycine N-methyltransferase* | 230 | 33111 | 7.1 | 34% | Metabolic enzyme regulates lipid and glucose homeostasis |
| E16 | HGD_MOUSE | Homogentisate 1,2-dioxygenase* | 123 | 50726 | 6.86 | 17% | Catalysis |
| E20 | Q9CPX4_MOUSE | Ferritin light chain 1* | 378 | 20817 | 5.66 | 65% | Iron metabolism |

*Up-regulated compared with the control group.
†Down-regulated compared with the matched group.

expression, however, was decreased in all γ-irradiated groups ($P<0.05$). NPM mRNA expression was increased in the 250 μGy/h irradiated group, when compared with controls ($P<0.05$), again findings that were consistent with proteomics analysis.

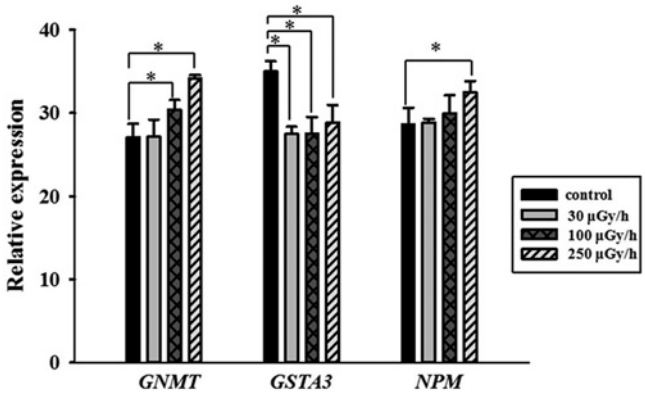


**Figure 4. qPCR verification of GNMT, GSTA3, and NPM gene expression in liver obtained from mice that were chronically exposed to 30, 100, and 250 μGy/h.**

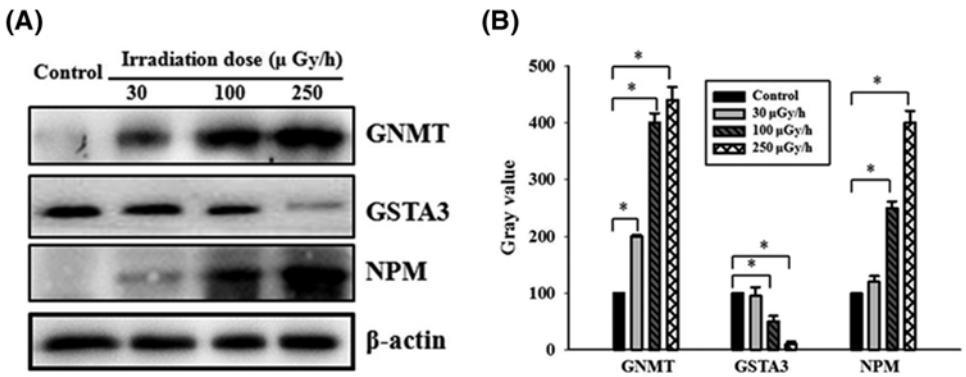


**Figure 5. WB verification of GNMT, GSTA3, and NPM expression in liver obtained from mice that were chronically exposed to 30, 100, and 250 μGy/h.**

(**A**) Representative WB of GNMT, GSTA3, and NPM expression in the liver tissues of mice treated with or without the indicated doses of irradiation (β-actin served as the internal control). (**B**) Quantification of GNMT, GSTA3, and NPM expression, evaluated by WB analysis. Values are presented as the mean ± S.D. from three experiments. We used *t* test to test the differences between groups and $^{*}P<0.05$ was considered significant.

Values are presented as the mean ± S.D. from three experiments. We used *t* test to test the differences between groups and $^{*}P< 0.05$ was considered significant.

## WB verification

We next performed WB studies to verify the γ-irradiation-dependent changes in the protein expression of GNMT, GSTA3, and NPM observed in our proteomics analysis. WB analysis revealed that, after 500 days of irradiation, GNMT and NPM protein expression was elevated and GSTA3 expression was decreased in liver tissues, when compared with controls (Figure 5). These changes in expression were consistent with the results of the proteomics analysis.

# Discussion

Humans are unavoidably exposed to low doses of radiation. Recently, increased attention has been given to biological effects of low dose rate or LDR on normal tissues. It is therefore desirable for radiation protection that low dose rate biomarkers be developed. The study of low dose and low dose rate provides guidance for radiation protection [25]. And the study of health effects of LDR is important for radiological protection research [26]. It follows that understanding the cellular responses to low dose rate is important. From previous studies it is known that it is difficult to detect an increase in DNA damage when the total cumulative dose is 400 times higher than the natural background and that doses are delivered at low dose rate. However, DNA damage can be easily measured when doses are delivered

*Bioscience Reports* (2018) **38** BSR20180536
https://doi.org/10.1042/BSR20180536

at high dose rate [27]. Another study showed that radiation genotoxicity depends on the dose rate [28]. Thus, dose rate is an important parameter to consider when developing radiation protection standards and for estimating risks.

Many researcher groups have provided fundamental data on the risk of ionizing radiation exposure for cancer development in humans [29]. The effects of LDR on an organism may include DNA damage and chromosome aberrations [30,31].

In our current study, we exposed mice to different doses of UT radiation for 500 days and then performed a proteomics analysis to identify possible changes in protein expression in the livers of the irradiated animals, given the observed effects of LDR on this organ. An analysis of differentially expressed proteins in cells and tissues under different conditions has previously proved useful in the identification of biomarkers associated with LDR [32,33].

We selected 29 protein spots based on the 2-DE gel image results for subsequent MALDI-TOF-MS analysis. Eighteen of these proteins were characterized successfully. Thirteen of the eighteen proteins related to low dose irradiation were up-regulated in the mouse liver and five were down-regulated. These data are summarized in Table 2. These proteins are related to detoxification, tumorigenesis, catalysis, cytoskeletal processes, and metabolism. Our research has shown that GNMT expression is enhanced in the liver tissues of mice following *in vivo* exposure to radiation originating from UT. GNMT is an important protein involved in folate metabolism, a process in which methionine and methylation play an important role [34]. In mammals, GNMT expression differs in various organs and tissues, suggesting that GNMT has tissue-specific roles. GNMT has been implicated in a variety of cancers. For example, it is down-regulated in almost all hepatocellular carcinoma (HCC) [35]; although abundantly expressed in the normal liver, GNMT expression is decreased in HCC tissues. GNMT deficiency is also associated with an inherited disorder of methionine metabolism [36]. Hepatic GNMT regulates lipid and glucose homeostasis, and its deficiency results in increased lipogenesis and triglycerides [37]. The overexpression of GNMT has been shown to prevent aflatoxin-induced carcinogenicity and to inhibit liver cancer cell proliferation. And the overexpression of GNMT provides insight into the development of insulin resistance through the modulation of the PI3K/Akt pathway [38]. The physiological role of GNMT can also provide insight into its connection with prostate cancer (PC) at various levels, including gene structure, gene expression, and metabolism. Moreover, GNMT plays an important role in controlling the methylation status of cells and in the metabolism of folic acid and methionine. During sarcosine treatment, GNMT expression in PC was observed to be affected slightly [39]. In our study we have shown that GNMT expression is altered following the 500-day irradiation with UT at all dose rates tested. GNMT can therefore be considered a promising target in the development of advanced diagnostic and/or prognostic techniques.

GSTA3 is a member of the glutathione S-transferase (GST) family, which is the most catalytically efficient steroid isomerase enzyme known in humans. GSTA3 plays an important role in the synthesis of steroid hormones [40-48], and it is selectively expressed in steroidogenic tissues. Mice GSTA3 mRNA levels were found to be elevated in animals after acute exposure to 8 Gy of $\gamma$-ray [49]. Given that this enzyme is a member of the GST family, this observation may reflect its radioprotective properties. In the present study, we found that GSTA3 expression was decreased in the three treatment groups exposed to different dose rates of UT irradiation. These results indicated that GSTA3 expression in the liver was altered in response to irradiation by UT.

NPM is mainly located in the nucleolus of cells and is an important protein implicated in many solid tumors. In the present study, NPM expression was found to be up-regulated in the experimental groups, when compared with the nonirradiated control group. In previous reports, NPM has been associated with tumor resistance and progression, and NPM silencing has been shown to significantly enhance the antitumor effects of baicalin, a natural component of the flowering plant, Scutellaria baicalensis Georgi [50]. NPM plays a role in promoting cancer, and its nucleolar localization is important for its cancer-promoting properties. Influencing the nucleolar-to-cytoplasmic distribution of this protein may therefore provide a potential strategy for HCC treatment [51]. NPM expression predicts recurrence and survival in upper tract urothelial carcinoma. High NPM expression significantly correlates with tumor location [52]. NPM is a multifunctional oligomeric phosphoprotein and is encoded by the *NPM1* gene [53,54]. NPM1mA is a mutant form of the NPM1 gene and is the most common genetic abnormality in patients with acute myeloid leukemia (AML) [55,56]. NPM1mA functions as an oncogene and is present in $\sim$30% of patients with AML [57]. Wild-type NPM1 is also frequently overexpressed in various tumors. NPM1 knockdown has been shown to significantly decrease nuclear factor-$\kappa$B-mediated invasion of breast cancer cells. Nuclear factor-$\kappa$B is a master regulator of inflammation [58]. Targeting NPM may provide a novel and effective method of reversing the effects of multidrug resistance, and this protein may be a potential adjuvant for tumor chemotherapy [59].

However, the biological effects of LDR are still unclear. The hazards associated with UT are numerous given its possible contribution to water pollution and acid rain, in addition to the internal risk that it can pose to the human body. Our study reveals that GNMT, GSTA3, and NPM are involved in the stress response induced in the liver tissues of mice following a 500-day exposure to less than or equal to 250 $\mu$Gy/h originating from UT.

## Funding

The present work was founded by the Defense Industrial Technology Development Program [grant number JCKY2016403C001]; National Natural Science Foundation of China [grant number U1401231]; China Postdoctoral Science Foundation [grant number 2014M562115]; and the Research Initiation Funding of University of South China for the Returned Scholars from Abroad [grant number 2014XQD46].

## Competing interests

The authors declare that there are no competing interests associated with the manuscript.

## Author contribution

D.D. designed the study. L.Y. contributed to study design, analyzed the data, and revised the manuscript. H.M. was responsible for collecting and analyzing the data, manuscript drafting, and final editing. N.H., J.S., and J.Y. had a role in data collection and analysis. K.D. and D.L. had a role in preparation of the manuscript.

## Abbreviations

2-DE, two-dimensional gel electrophoresis; AML, acute myeloid leukemia; BCA, bicinchoninic acid; GNMT, glycine N-methyltransferase; GST, glutathione S-transferase; GSTA3, glutathione S-transferase A3; HCC, hepatocellular carcinoma; IPI, international protein index; LDR, low dose radiation; MALDI-TOF-MS, matrix-assisted laser desorption/ionization time of flight mass spectrometry; NPM, nucleophosmin; PC, prostate cancer; PCR, polymerase chain reaction; PI3K/Akt, phosphatidylinositol-3 kinase/Akt; PMF, peptide mass fingerprinting; PVDF, polyvinylidene fluoride; S.D., standard deviation; RT, real-time; TBST, tris-buffered saline–0.1% Tween 20; UT, uranium tailings; WB, Western blotting.

# References

1 Lian, Y., Xiao, J., Ji, X. et al. (2015) Protracted low-dose radiation exposure and cataract in a cohort of Chinese industry radiographers. *Occup. Environ. Med.* **72**, 640–647, https://doi.org/10.1136/oemed-2014-102772
2 Roch-Lefèvre, S., Martin-Bodiot, C., Grégoire, E. et al. (2016) A mouse model of cytogenetic analysis to evaluate caesium137 radiation dose exposure and contamination level in lymphocytes. *Radiat. Environ. Biophys.* **55**, 61–70, https://doi.org/10.1007/s00411-015-0620-7
3 Brooks, A.L. and Dauer, L.T. (2014) Advances in radiation biology: effect on nuclear medicine. *Semin. Nucl. Med.* **44**, 179–186, https://doi.org/10.1053/j.semnuclmed.2014.03.004
4 Edin, N.J., Christoffersen, S., Fenne, S. et al. (2015) Cell inactivation by combined low dose-rate irradiation and intermittent hypoxia. *Int. J. Radiat. Biol.* **91**, 336–345, https://doi.org/10.3109/09553002.2014.996262
5 Bang, H.S., Choi, M.H., Kim, C.S. et al. (2016) Gene expression profiling in undifferentiated thyroid carcinoma induced by high-dose radiation. *J. Radiat. Res.* **57**, 238–249, https://doi.org/10.1093/jrr/rrw002
6 Mancuso, M., Pasquali, E., Braga-Tanaka, III, I. et al. (2015) Acceleration of atherogenesis in ApoE-/- mice exposed to acute or low-dose-rate ionizing radiation. *Oncotarget* **6**, 31263–31271, https://doi.org/10.18632/oncotarget.5075
7 Kempf, S.J., Janik, D., Barjaktarovic, Z. et al. (2016) Chronic low-dose-rate ionising radiation affects the hippocampal phosphoproteome in the ApoE-/- Alzheimer's mouse model. *Oncotarget* **7**, 71817–71832, https://doi.org/10.18632/oncotarget.12376
8 Jiang, X., Hong, Y., Zhao, D. et al. (2017) Low dose radiation prevents doxorubicin-induced cardiotoxicity. *Oncotarget* **9**, 332–345
9 Zhou, L., Zhang, X., Li, H. et al. (2018) Validating the pivotal role of the immune system in low-dose radiation-induced tumor inhibition in Lewis lung cancer-bearing mice. *Cancer Med.* **7**, 1338–1348
10 Yin, L., Wang, P., Wen, T. et al. (2017) Synthesis of layered titanate nanowires at low temperature and their application in efficient removal of U(VI). *Environ. Pollut.* **226**, 125–134, https://doi.org/10.1016/j.envpol.2017.03.078
11 Li, Z.J., Huang, Z.W., Guo, W.L. et al. (2017) Enhanced photocatalytic removal of Uranium(VI) from aqueous solution by magnetic TiO2/Fe3O4 and Its graphene composite. *Environ. Sci. Technol.* **51**, 5666–5674, https://doi.org/10.1021/acs.est.6b05313
12 Wang, J., Liu, J., Zhu, L. et al. (2012) Uranium and thorium leached from uranium mill tailing of Guangdong Province, China and its implication for radiological risk. *Radiat. Prot. Dosimetry* **152**, 215–219, https://doi.org/10.1093/rpd/ncs229
13 Skipperud, L., Strømman, G., Yunusov, M. et al. (2013) Environmental impact assessment of radionuclide and metal contamination at the former U sites Taboshar and Digmai, Tajikistan. *J. Environ. Radioact.* **9**, 50–62, https://doi.org/10.1016/j.jenvrad.2012.05.007
14 Brulfert, F., Safi, S., Jeanson, A. et al. (2017) Enzymatic activity of the CaM-PDE1 system upon addition of actinyl ions. *J. Inorg. Biochem.* **172**, 46–54, https://doi.org/10.1016/j.jinorgbio.2017.04.007
15 Yan, X. and Luo, X. (2015) Radionuclides distribution, properties, and microbial diversity of soils in uranium mill tailings from southeastern China. *J. Environ. Radioact.* **139**, 85–90, https://doi.org/10.1016/j.jenvrad.2014.09.019
16 Wise, J.T.F., Wang, L., Zhang, Z. et al. (2017) The 9th conference on metal toxicity and carcinogenesis: the conference overview. *Toxicol. Appl. Pharmacol.* **331**, 1–5
17 Mesri, M. (2014) Advances in proteomic technologies and its contribution to the field of cancer. *Adv. Med.* **2014**, 238045
18 Napoli, C., Zullo, A., Picascia, A. et al. (2013) Recent advances in proteomic technologies applied to cardiovascular disease. *J. Cell. Biochem.* **114**, 7–20, https://doi.org/10.1002/jcb.24307

19 Nicolaou, O., Kousios, A., Hadjisavvas, A. et al. (2017) Biomarkers of systemic lupus erythematosus identified using mass spectrometry-based proteomics: a systematic review. *J. Cell. Mol. Med.* **21**, 993–1012, https://doi.org/10.1111/jcmm.13031
20 Miah, S., Banks, C.A., Adams, M.K. et al. (2016) Advancement of mass spectrometry-based proteomics technologies to explore triple negative breast cancer. *Mol. Biosyst.* **13**, 42–55, https://doi.org/10.1039/C6MB00639F
21 Aslam, B., Basit, M., Nisar, M.A. et al. (2017) Proteomics: technologies and their applications. *J. Chromatogr. Sci.* **55**, 182–196, https://doi.org/10.1093/chromsci/bmw167
22 Yi, L., Hu, N., Yin, J. et al. (2017) Up-regulation of calreticulin in mouse liver tissues after long- term irradiation with low-dose-rate gamma rays. *PLoS ONE* **12**, e0182671, https://doi.org/10.1371/journal.pone.0182671
23 Yi, L., Li, L., Yin, J., Hu, N., Li, G. and Ding, D. (2016) Proteomics analysis of liver tissues from C57BL/6J mice receiving low-dose 137Cs radiation. *Environ. Sci. Pollut. Res. Int.* **23**, 2549–2556, https://doi.org/10.1007/s11356-015-5494-3
24 Hu, Y., Yang, L., Yang, H., He, S. and Wei, J.F. (2017) Identification of snake venom allergens by two-dimensional electrophoresis followed by immunoblotting. *Toxicon* **125**, 13–18, https://doi.org/10.1016/j.toxicon.2016.11.251
25 Boice, Jr, J.D. (2017) Space: the final frontier-research relevant to Mars. *Health Phys.* **112**, 392–397, https://doi.org/10.1097/HP.0000000000000656
26 Madas, B.G. (2016) Radon exposure and the definition of low doses-the problem of spatial dose distribution. *Health Phys.* **111**, 47–51, https://doi.org/10.1097/HP.0000000000000516
27 Brooks, A.L., Hoel, D.G. and Preston, R.J. (2016) The role of dose rate in radiation cancer risk: evaluating the effect of dose rate at the molecular, cellular and tissue levels using key events in critical pathways following exposure to low LET radiation. *Int. J. Radiat. Biol.* **92**, 405–426, https://doi.org/10.1080/09553002.2016.1186301
28 Graupner, A., Eide, D.M., Brede, D.A. et al. (2017) Genotoxic effects of high dose rate X-ray and low dose rate gamma radiation in ApcMin/+ mice. *Environ. Mol. Mutagen.* **58**, 560–569, https://doi.org/10.1002/em.22121
29 Kron, T., Lehmann, J. and Greer, P.B. (2016) Dosimetry of ionising radiation in modern radiation oncology. *Phys. Med. Biol.* **61**, 167–205, https://doi.org/10.1088/0031-9155/61/14/R167
30 Piotrowski, I., Kulcenty, K., Suchorska, W.M. et al. (2017) Carcinogenesis induced by low-dose radiation. *Radiol. Oncol.* **51**, 369–377, https://doi.org/10.1515/raon-2017-0044
31 Feinendegen, L.E. (2005) Evidence for beneficial low level radiation effects and radiation hormesis. *Br. J. Radiol.* **78**, 3–7, https://doi.org/10.1259/bjr/63353075
32 Bakshi, M.V., Barjaktarovic, Z., Azimzadeh, O. et al. (2013) Long-term effects of acute low-dose ionizing radiation on the neonatal mouse heart: a proteomic study. *Radiat. Environ. Biophys.* **52**, 451–461, https://doi.org/10.1007/s00411-013-0483-8
33 Bakshi, M.V., Azimzadeh, O., Barjaktarovic, Z. et al. (2015) Total body exposure to low-dose ionizing radiation induces long-term alterations to the liver proteome of neonatally exposed mice. *J. Proteome Res.* **14**, 366–373, https://doi.org/10.1021/pr500890n
34 Beagle, B., Yang, T.L., Hung, J. et al. (2005) The glycine N-methyltransferase (GNMT) 1289 C->T variant influences plasma total homocysteine concentrations in young women after restricting folate intake. *J. Nutr.* **135**, 2780–2785, https://doi.org/10.1093/jn/135.12.2780
35 Li, C.H., Yen, C.H., Chen, Y.F. et al. (2017) Characterization of the GNMT-HectH9-PREX2 tripartite relationship in the pathogenesis of hepatocellular carcinoma. *Int. J. Cancer* **140**, 2284–2297, https://doi.org/10.1002/ijc.30652
36 Barić, I., Erdol, S., Saglam, H. et al. (2017) Glycine N-methyltransferase deficiency: a member of dysmethylating liver disorders? *JIMD Rep.* **31**, 101–106, https://doi.org/10.1007/8904˙2016˙543
37 Kant, R., Yen, C.H., Lu, C.K. et al. (2016) Identification of 1,2,3,4,6-Penta-O-galloyl-β-d-glucopyranoside as a glycine N-methyltransferase enhancer by high-throughput screening of natural products inhibits hepatocellular carcinoma. *Int. J. Mol. Sci.* **17**, e669, https://doi.org/10.3390/ijms17050669
38 Liao, Y.J., Lee, T.S., Twu, Y.C. et al. (2016) Glycine N-methyltransferase deficiency in female mice impairs insulin signaling and promotes gluconeogenesis by modulating the PI3K/Akt pathway in the liver. *J. Biomed. Sci.* **23**, 69, https://doi.org/10.1186/s12929-016-0278-8
39 Heger, Z., Merlos Rodrigo, M.A., Michalek, P. et al. (2016) Sarcosine up-regulates expression of genes involved in cell cycle progression of metastatic models of prostate cancer. *PLoS ONE* **11**, e0165830, https://doi.org/10.1371/journal.pone.0165830
40 Musdal, Y., Hegazy, U.M., Aksoy, Y. et al. (2013) FDA-approved drugs and other compounds tested as inhibitors of human glutathione transferase P1-1. *Chem. Biol. Interact.* **205**, 53–62, https://doi.org/10.1016/j.cbi.2013.06.003
41 Dourado, D.F., Fernandes, P.A., Mannervik, B. et al. (2014) Isomerization of Δ5-androstene-3,17-dione into Δ4-androstene-3,17-dione catalyzed by human glutathione transferase A3-3: a computational study identifies a dual role for glutathione. *J. Phys. Chem. A* **118**, 5790–5800, https://doi.org/10.1021/jp410810q
42 Fedulova, N., Raffalli-Mathieu, F. and Mannervik, B. (2010) Porcine glutathione transferase alpha 2-2 is a human GST A3-3 analogue that catalyses steroid double-bond isomerization. *Biochem. J.* **431**, 159–167, https://doi.org/10.1042/BJ20100839
43 Ing, N.H., Forrest, D.W., Riggs, P.K. et al. (2014) Dexamethasone acutely down-regulates genes involved in steroidogenesis in stallion testes. *J. Steroid Biochem. Mol. Biol.* **143**, 451–459, https://doi.org/10.1016/j.jsbmb.2014.07.003
44 Matsumura, T., Imamichi, Y., Mizutani, T. et al. (2013) Human glutathione S-transferase A (GSTA) family genes are regulated by steroidogenic factor 1 (SF-1) and are involved in steroidogenesis. *FASEB J.* **27**, 3198–3208, https://doi.org/10.1096/fj.12-222745
45 Larsson, E., Mannervik, B. and Raffalli-Mathieu, F. (2011) Quantitative and selective polymerase chain reaction analysis of highly similar human alpha-class glutathione transferases. *Anal. Biochem.* **412**, 96–101, https://doi.org/10.1016/j.ab.2011.01.024
46 Faucette, A.N., Maher, V.A., Gutierrez, M.A. et al. (2014) Temporal changes in histomorphology and gene expression in goat testes during postnatal development. *J. Anim. Sci.* **92**, 4440–4448, https://doi.org/10.2527/jas.2014-7903
47 Robertson, G.J., Stoychev, S.H., Sayed, Y. et al. (2017) The effects of mutating Tyr9 and Arg15 on the structure, stability, conformational dynamics and mechanism of GSTA3-3. *Biophys. Chem.* **5**, 40–48, https://doi.org/10.1016/j.bpc.2017.02.004

48 Mizutani, T., Ishikane, S., Kawabe, S. et al. (2015) Transcriptional regulation of genes related to progesterone production. *Endocr. J.* **62**, 757–763, https://doi.org/10.1507/endocrj.EJ15-0260
49 Kim, I.S.G., Nam, S.Y. and Kim, C.W. (1998) *In vivo* radioprotective effects of oltipraz in gamma-irradiated mice.. *Biochem. Pharmacol.* **55**, 1585–1590, https://doi.org/10.1016/S0006-2952(97)00669-2
50 Li, D., Lin, B., Yusuf, N. et al. (2017) Proteomic analysis and functional studies of baicalin on proteins associated with skin cancer. *Am. J. Chin. Med.* **45**, 599–614, https://doi.org/10.1142/S0192415X17500355
51 Li, X., Xu, D.H., Liu, F. et al. (2017) Relocation of NPM affects the malignant phenotypes of hepatoma SMMC-7721 cells. *J. Cell. Biochem.* **118**, 3225–3236, https://doi.org/10.1002/jcb.25971
52 Sawazaki, H., Ito, K., Asano, T. et al. (2016) Increased nucleophosmin expression is a strong predictor of recurrence and prognosis in patients with N0M0 upper tract urothelial carcinoma undergoing radical nephroureterectomy. *World J. Urol.* **35**, 1081–1088, https://doi.org/10.1007/s00345-016-1977-1
53 Lin, J., Hisaoka, M., Nagata, K. et al. (2016) Functional characterization and efficient detection of Nucleophosmin/NPM1 oligomers. *Biochem. Biophys. Res. Commun.* **480**, 702–708, https://doi.org/10.1016/j.bbrc.2016.10.125
54 Zhang, S., Qin, F., Yang, L. et al. (2016) Nucleophosmin mutations induce chemosensitivity in THP-1 leukemia cells by suppressing NF-κB activity and regulating Bax/Bcl-2 expression. *J. Cancer* **7**, 2270–2279, https://doi.org/10.7150/jca.16010
55 Brodská, B., Kráčmarová, M., Holoubek, A. et al. (2017) Localization of AML-related nucleophosmin mutant depends on its subtype and is highly affected by its interaction with wild-type NPM. *PLoS ONE* **12**, e0175175, https://doi.org/10.1371/journal.pone.0175175
56 Nabbouh, A.I., Hleihel, R.S., Saliba, J.L. et al. (2017) Imidazoquinoxaline derivative EAPB0503: a promising drug targeting mutant nucleophosminv1 in acute myeloid leukemia. *Cancer* **123**, 1662–1673, https://doi.org/10.1002/cncr.30515
57 Andresen, V., vErikstein, B.S., Mukherjee, H. et al. (2016) Anti-proliferative activity of the NPM1 interacting natural product avrainvillamide in acute myeloid leukemia. *Cell Death Dis.* **7**, e2497, https://doi.org/10.1038/cddis.2016.392
58 Lin, J., Kato, M., Nagata, K. et al. (2016) Efficient DNA binding of NF-κB requires the chaperone-like function of NPM1. *Nucleic Acids Res.* **45**, 3707–3723
59 Luo, F., Li, H., Liang, J. et al. (2017) Downregulation of NPM reverses multidrug resistance in human hepatoma cells via inhibition of P-glycoprotein expression. *Mol. Med. Rep.* **15**, 2360–2368, https://doi.org/10.3892/mmr.2017.6246